Sparse Models and Pursuit Algorithms for PIV Tomography

Ioana Barbu, Cédric Herzet, Etienne Mémin

Sparse Models and Pursuit Algorithms for PIV Tomography

Ioana Barbu[1,a], Cédric Herzet[1], and Etienne Memin[1]

Fluminance, INRIA Centre Rennes - Bretagne Atlantique, Rennes

Abstract. The goal of this article is to study the performance of pursuit algorithms when applied to the tomographic problem of particle reconstruction.

1 Introduction

The *Tomographic Particle Image Velocimetry (TomoPIV)* is an experimental technique for the retrieval of Eulerian velocity measurements of turbulent fluids introduced in [1]. The technique aims at reconstructing, with very high update rates, 3D motion fields of lightly seeded particles from the images captured by a finite number of cameras.

A crucial step in solving the velocity fields is estimating **the volume distribution** of the seeded particles. However, the number of observations available for the reconstruction is very limited, which implies solving an underdetermined linear system. In order to cope with the ambiguities related to the behavior of these systems, methods in the current literature exploit prior knowledge on the 3D signal, which is **non-negative** [2] and **sparse** [3]. While the state of the art algorithms lead to acceptable reconstruction with respect to accuracy, they each present specific drawbacks: they either induce too dense positive solutions or suffer from high-complexity without guaranteeing non-negative solutions. Our current investigation focuses on reconstructing a sparse volumetric signal from few projections with respect to accuracy and complexity. In order to achieve a precise sparse signal with a reasonable computational time, we took an interest in a family of algorithms for sparse representations extensively known as **pursuit algorithms**. By applying them to our reconstruction problem, we point out a faster alternative to the state-of-the-art techniques for comparable performance in terms of probability of correct reconstruction for low densities of particles.

2 Related Models

Let us describe the mathematical algebraic image reconstruction model relating the image data to the sought particle density, commonly adopted in the TomoPIV analysis. We denote by $\mathcal{V} \subset \mathbb{R}^3$ the cuboid of interest in the considered three-dimensional space, partitioned into a cartesian grid of cubic **vo**lume **el**ements (voxels) $\zeta_j \subset \mathbb{R}^3$ of volume $\text{vol}(\zeta_j) \triangleq \int_{\zeta_j} 1 \, d\mathbf{z}$ such that

$$\bigcup_{j=1}^{m} \zeta_j = \mathcal{V}, \qquad \bigcap_{j=1}^{m} \zeta_j = \varnothing. \tag{1}$$

Our goal is to recover the volumetric intensity distribution, say $I(\mathbf{z})$, $\forall\, \mathbf{z} \in \mathcal{V}$ from a vector of measures $\mathbf{y}$ made up of a set of pixels collected from a synchronized multi-camera system. Following the

[a] e-mail: ioana.barbu@inria.fr

classical projection paradigm, the i^{th} element of $\mathbf{y}$ then writes:

$$y_i = \int_{\Omega_i} I(\mathbf{z})\, d\mathbf{z}, \tag{2}$$

where Ω_i is the cone of light originated from the camera optical center and passing through the boundaries of the i^{th} pixel. Note that any physically-consistent intensity distribution $I(\mathbf{z})$ must correspond to a finite-energy signal, *i.e.*, $I(\mathbf{z}) \in \mathcal{L}^2(\mathcal{V})$. In the sequel, we will moreover assume that $I(\mathbf{z})$ belongs to a finite-dimensional subspace of $\mathcal{L}^2(\mathcal{V})$. Let $\{b_j(\mathbf{z})\}_{j=1}^m$ be an orthogonal basis of this subspace. $I(\mathbf{z})$ can then be rewritten as

$$I(\mathbf{z}) = \sum_{j=1}^{m} x_j\, b_j(\mathbf{z}). \tag{3}$$

where $x_j = \int_{\mathcal{V}} I(\mathbf{z})\, b_j(\mathbf{z}) d\mathbf{z}$. In this paper, we assume that $b_j(\mathbf{z})$'s are defined as rectangular-pulse functions, expressed as:

$$b_j(\mathbf{z}) \triangleq \begin{cases} 1/\mathrm{vol}(\zeta_j), & \text{if } \mathbf{z} \in \zeta_j, \\ 0, & \text{otherwise.} \end{cases} \tag{4}$$

Coming back to (3) and integrating the j^{th} basis function along the i^{th} cone of sight gives us the coefficients:

$$d_{ij} \triangleq \int_{\Omega_i} b_j(\mathbf{z}) d\mathbf{z} = \frac{1}{\mathrm{vol}(\zeta_j)} \int_{\Omega_i \cap \zeta_j} 1\, d\mathbf{z}. \tag{5}$$

The integral in the right-hand side of (5) represents the volume of the intersection of the i^{th} cone of sight Ω_i with the j^{th} voxels ζ_j. It can be easily evaluated by means of a numerical integration method. Then, using (3) and (5), our model can be described by a system of linear equations:

$$y_i = \sum_{j=1}^{m} x_j d_{ij} \text{ expressed in matrix formulation as: } \mathbf{y} = \mathbf{D}\mathbf{x}, \tag{6}$$

where $\mathbf{y}$ is the measurement vector, $\mathbf{D} \in \mathbb{R}^{n \times m}$ is a dictionary collecting the elements defined in (5) and $\mathbf{x} \in \mathbb{R}^m$ is a vector made up of the unknown projection coefficients x_j.

3 Low-complexity Pusuit for TomoPIV

Before going through the discussion on low-complexity procedures for the TomoPIV problem, we first review the main approaches available in the literature. The choice of estimation paradigms employed within the TomoPIV community has been influenced by specific features of the system (6); in a nutshell, we most often deal with an **underdetermined linear system** ($n < m$) and a **non-negative sparse** vector $\mathbf{x}$ to be reconstructed.

A classical solution in the TomoPIV literature exploiting the non-negativity of $\mathbf{x}$ is the so-called *MART (Multiplicative Algebraic Reconstruction Technique)*, which addresses the following optimization problem:

$$\mathbf{x}^\star = \arg\min_{\mathbf{x}} \left\{ \sum_{j=1}^{m} x_j \log x_j \right\} \text{ subject to } \begin{cases} \mathbf{x} \geq 0 \\ \mathbf{D}\mathbf{x} = \mathbf{y}. \end{cases} \tag{7}$$

The first constraint forces the non-negativity of the solution whereas the second one ensures its compatibility with the observed vector $\mathbf{y}$. MART looks for a solution of this problem by means of an iterative scheme based on a closed-form formula.

A more recent approach to address the TomoPIV reconstruction problem revolves around sparse representations (SR). The idea consists in exploiting the sparsity of the sought vector $\mathbf{x}$ to remove the ambiguity of the solution. More formally, the considered optimization problem writes

$$\mathbf{x}^* = \arg\min_{\mathbf{x}} \|\mathbf{x}\|_0 \text{ subject to } \mathbf{D}\mathbf{x} = \mathbf{y}, \tag{8}$$

where $\|\mathbf{x}\|_0$ denotes the ℓ_0 pseudo-norm which counts the number of nonzero elements in $\mathbf{x}$. Solving (8) is therefore tantamount to finding the vector with the minimum number of nonzero elements satisfying the observation model (6). Unfortunately, problem (8) is NP-hard. In practice, we need to resort to heuristic algorithms to access to its solutions. Therefore, numerous suboptimal (but tractable) algorithms have been devised in the literature to cope with the SR problem. One can distinguish between 2 main families.

The algorithms based on a problem relaxation consist in approximating the non-convex and non-smooth l_0 norm by its corespondent l_1 norm. The problem can therefore be solved efficiently by standard optimization procedures. This family refers to basis pursuit (BP)[9] and Global Matching Filter (GMF)[5]. In the context of TomoPIV, several papers have presented this option ([3], [6]), displaying convincing results in terms of accuracy of approximation *vs* sparsity, at the price of a rather elevated complexity. The second category comprises **the pursuit algorithms**. These procedures aim at solving (8) by making a succession of locally-optimal decisions on the support vector of the sparse decomposition, *i.e.*, by sequentially adding or removing locally-optimal atom(s) in order to build up the sparse vector $\mathbf{x}$. Within the family of pursuit algorithms, one can distinguish between several approaches by the way they chose the support vector of the sparse decomposition and/or the way they compute the coefficients of the chosen atoms. We mention Orthogonal MP (OMP) [7], or Subspace Pursuit (SP)[8] algorithms. These standard pursuit algorithms have been recently extended in a Bayesian content. When expressing the sparse representation problem as the solution of a Bayesian inference problem, one can apply statistical tools to solve it. We allude to the *bayesian pursuit procedures*, such as Bayesian OMP (BOMP) and Bayesian SP (BSP) – all in [9]. Unlike their standard counter-part, these Bayesian pursuit algorithms allow for atom deselection. For greedy strategies such as OMP and BOMP the coefficient update stage relies on the costly computation of a pseudo-inverse. In [10] improvements have been proposed to approximate the latter with a gradient based scheme. We refer to these novel procedures as dOMP and dBOMP. We concentrate our analysis on the last-mentioned paradigm, that aims at solving a sparsity-orientated criterion and show the study of its performance in a TomoPIV context.

4 Results

We consider a cuboid of size $100\times100\times50$ *mm* partitioned into a cartesian grid of $21\times21\times11$ voxels. The origin of the world frame is chosen in the center of the cuboid. The volume projects simultaneously into four 33×33 pixels CCD sensors, each sized 8×8 *mm*. The optical axe of each camera is defined by the vector joining the origin of the world frame and its optical center and points towards the cuboid. The optical centers are placed such that the extreme edges of the cuboid all project at once into each camera's image screen such that the cuboid's silhouette is in the visibility field of each sensor.The projection into the image screen is realized by approximating each voxel by $3\times3\times3$ sub-voxels. We choose the focal distance of each sensor $f = 4$ *mm*. After eliminating from the observation vector the pixels that don't capture any of the voxels, we obtain a dictionary of dimension 2433×4851. We seed the volume with increasing number of particles, at randomly chosen positions at grid-points, going from 50 to 450 seeds. For each one of these values, we launch 200 experiences, that we average.

We observe in Fig.1(a) that, for low sparsity levels, the percentage of correct reconstruction for the pursuit algorithms is comparable to the performances of state of the art MART and BP. For this particular range of density levels, these performances are realized in lower computational time. We refer to Fig. 1(b) in order to observe that while OMP is considerably more complex than MART and BP, the other pursuit algorithms enhance the rapidity with a factor going from 10 to 100. We point out the incontestable improvements in computational time brought by the directional approach to the classical OMP and BOMP. Fig.1(c) and Fig.1(d) represent the algorithm performance for the reconstruction of the SR support. We can observe that KBOMP, BSP, BOMP and dBOMP succeed in keeping both small missed detection and false detection rates on the entire range of the sparsity levels. This is not the case for the other algorithms. Since MART and BP produce quite dense solutions, they generally select all the "good" atoms (*e.g.*, for this experience, their respective missed detection rates are null), *i.e.*, the atoms having been used to generate the data, but this is performed at the expense of a high false detection rate.

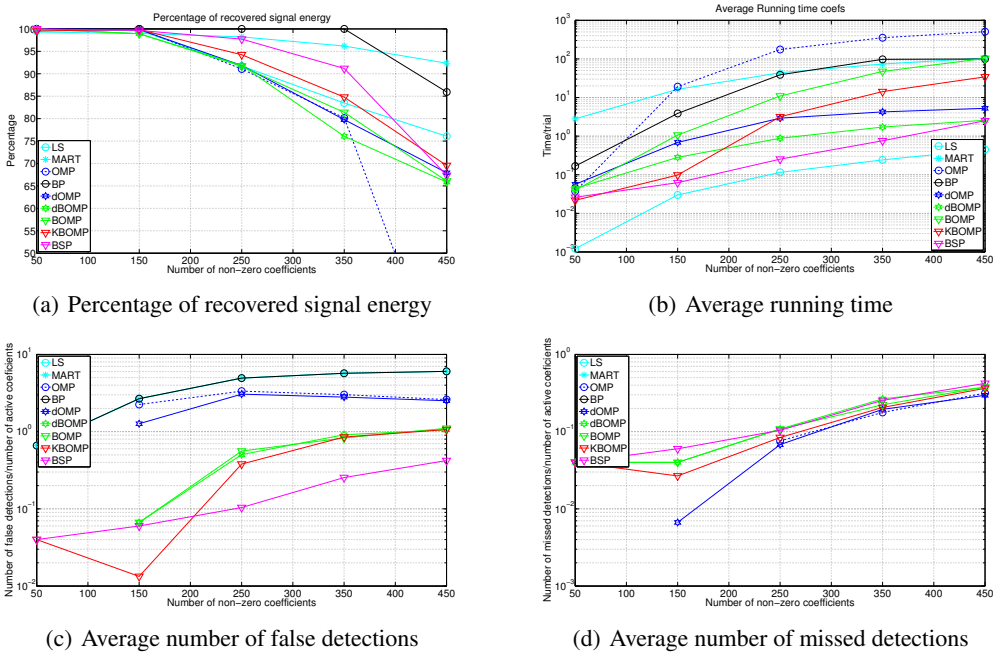

(a) Percentage of recovered signal energy

(b) Average running time

(c) Average number of false detections

(d) Average number of missed detections

Fig. 1. SR reconstruction performance versus number of nonzero coefficients

5 Conclusions

We have expressed the problem of TomoPIV into a sparse representation context and empirically investigated upon the behavior of pursuit algorithms for the reconstruction of the 3D signal compared to state of the art basis pursuit and algebraic methods. We have pointed out that, for low density levels, the pursuit algorithms have comparable performance with respect to percentage of recovered signal, for lower computational time. We suggest KBOMP and BSP as the best compromise between complexity and accuracy. However, the results shown correspond to a particular scenario and can vary under different sensor configurations, for a different number of cameras.

References

1. G. Elsinga, F. Scarano, B. Wieneke, and B. van Oudheusden, Exp. in Fluids **41**, (2006) 933–947
2. R. Gordon, R. Bender, and G. T. Herman, Jour. of theoretical biology **29**, (1970) 471–481
3. S. Petra, C. Schnörr, A. Schröder, and B. Wieneke, In Proc. Workshop on Math. Modeling Environ., **27**, (2007)
4. S. Chen, D. L. Donoho, and M. A. Saunders, SIAM Jour. Scientific Computing **20**, (1998) 33-61
5. J.-J. Fuchs, IEEE Trans. Signal Process **49**, (2001) 702-709
6. S. Petra, A.Schröder, B. Wieneke, and C.Schnörr, Notes on Numerical Fluid Mechanics and Multidisciplinary Design - Imaging Measurement Methods for Flow Analysis **106**, (2009) 471–481
7. Y. C. Pati, R. Rezaiifar and P. S. Krishnaprasad, In Proc. Asilomar Conference on Signals, Systems, and Computers, **27**, (1993) 40-44
8. W. Dai and O. Milenkovic, CoRR, (2008)
9. C. Herzet and A. Drémeau, in Proc. European Signal Processing Conference, (2010)
10. T. Blumensath and M. E. Davies, IEEE Trans. Signal Process **56**, (2008) 2370-2382